INELASTIC DISPLACEMENT RATIOS OF SSI SYSTEMS

Ertugrul DEMIROL[1] and Ashraf S. AYOUB[2]

Abstract

This paper presents the effect of soil-structure interaction on seismic inelastic displacement ratios of Single Degree of Freedom (SDOF) systems. Existing methods used in the past assumes the soil to be rigid. Through simplified equivalent fixed-base methods, the effect of soil-structure interaction (SSI) on the inelastic behaviour of structures is evaluated for different soil parameters using effective period and damping values. Using a degrading modified Clough model, the influence of different types of degradation is accounted for, for SDOF systems with periods ranging from 0.2-1.4 sec. In total 300 different earthquake motions recorded on firm soil condition with magnitudes greater than 5 and peak ground acceleration (PGA) values greater than 0.08g were selected. These records were scaled to the same hazard level and applied on five experimentally-tested reinforced concrete columns selected from the Pacific Earthquake Engineering Research Center database. A total of 384,000 dynamic analyses were conducted. The results of the soil interacting systems are compared with the fixed-base case for different strength reduction factors (R) and foundation aspect ratios (h/r) for a range of NEHRP soil types C and D properties. These results show that the maximum inelastic displacements for soil type D are greater than those of soil type C and the fixed-base case. Particularly for periods less than 0.6s with large aspect ratios, the effects of soil-structure interaction should be accounted for. Finally, the collected data was used to derive mathematical expressions for inelastic displacement ratios of SSI systems, suitable for use in performance-based seismic evaluation of structures.

Key Words: Soil Structure Interaction, SSI, Inelastic Displacement Ratio, Inelastic Ratio, Degradation.

---

[1] Department of Civil Eng., City, University of London, London, UK, Ertugrul.Demirol.1@city.ac.uk
[2] Department of Civil Eng., City, University of London, London, UK, Ashraf.Ayoub.1@city.ac.uk

1 Introduction

Most common seismic codes used in design practice assume the base of the foundation to be fixed, which does not account for the effect of SSI. This study attempts to include the effect of SSI in performance based seismic design codes using simplified equivalent single degree of freedom (SDOF) systems.

In earthquake design, the maximum displacement of a structure under seismic excitations is typically calculated using inelastic displacement ratios. However, currently adopted methods do not account for the effect of SSI, and do not consider degradation effects or this effect is not correctly defined. This paper investigates the effect of SSI on the inelastic response of structures using energy-based degradation models, which account for four types of degradation. Five specimens representative of reinforced concrete (RC) structures are selected for analysis amongst the tested columns in the Pacific Earthquake Engineering Research centre (PEER) database [1]. The analysis was conducted using similar parameters to those reported in [2] for consistency and accuracy. A database of 300 earthquake records on firm sites selected by Ozkul in [3] is used in this study to increase the statistical importance of the results. The selection process of the data was based on earthquakes with magnitudes greater than 5 and peak ground acceleration (PGA) values ranging from 0.8g-2.73g. Different soil profiles with effective period and damping values differing from the fixed-base case were compared for different strength reduction factors ranging from $R = 1.5$-8.

The inelastic displacement ratio used in seismic design is defined as the relationship between maximum inelastic displacement and maximum elastic displacement of SDOF systems. Veletsos and Newmark [4] conducted the first study on this topic in 1960 using three-earthquake ground motions. The results show the maximum inelastic displacement is approximately equivalent to the maximum elastic displacement, also known as the "equal displacement rule", for periods in the low frequency range. This study also showed that in high frequency range this rule is not valid as the inelastic displacement values are greater than their elastic counterparts.

2

Shimazaki and Sozen [5] identified that the equal displacement rule applies to periods of vibration higher than the "characteristic period"; this is known as the period between the short period range and the limiting periods of the response spectra, regardless of which hysteric model used. Recently, Miranda [6] used 264 ground motions to compute the constant ductility inelastic displacement ratios of an SDOF system on firm sites using a series of new simplified functions. He also established that neither the earthquake magnitude nor the epicenter distance affects the inelastic displacement ratio. In addition to this, the findings also show for soil types with shear wave velocity greater than 180 m/s, the effect of ground conditions are small and therefore can be neglected in seismic design.

Miranda [6] also developed a new equation that estimated the inelastic displacement ratios of SDOF systems as a function of ductility ratio and period of vibration. Furthermore, Ruiz-Garcia and Miranda [7] evaluated the behavior of existing structures built on firm sites using the simplified functions of [6]. The inelastic displacement ratios were estimated through evaluating the periods of vibration, level of lateral yielding strength, site conditions, earthquake magnitude, distance to the source and the strain-hardening ratio. This simplified equation became very useful in preliminary design of new structures; however for existing structures the results of the study show that inelastic displacement ratios underestimate the expected maximum lateral deformations in systems with lateral strength previously known.

Similarly, Nassar and Krawinkler [8] performed analysis on SDOF systems using a smaller set of earthquake records to estimate the inelastic displacement ratios considering the degradation effects with a bilinear, Clough and pinching models. Halabian [9] studied the effect of SSI on the seismic behavior and design of large structures built on soft soils.

Chopra and Chintanapakdee [10] developed two different equations for calculating the inelastic displacement ratios for new and existing structures with 214 earthquake records; however, this model disregarded the effect of degradation.

More recently, Chenouda and Ayoub [11-12] and Ayoub and Chenouda [13] proposed a new energy-based model which accounts for four types of degradation: strength, unloading

3

stiffness, accelerated stiffness, and cap degradation. The dynamic analysis also shows predictions of structural collapse for SDOF systems subjected to earthquake loading.

Eser et al. [14] attempted to calculate the inelastic displacement ratios of soil interacting systems with effective periods and effective damping values differing from the fixed-base. The Newmark method for step-by-step time integration was used in the analysis with proposed equations for estimating the inelastic deformation of structures. Aydemir [15] also studied soil interacting systems using a modified Clough model, and developed an equation for estimating the inelastic deformation of existing structures with lateral strength previously known. However, this work did not account for the effect of degradation. Another study by Khoshnoudian et al. [16] derives estimates of inelastic displacements for SSI bilinear non-degrading systems using a set of 20 earthquake records. On the other hand, Allotey and El Naggar [17] developed a beam on Winkler foundation model that accounts for the rocking response of foundation through specified analytical moment-rotation curves. The model was extended to account for the coupling effect of vertical, horizontal and rocking response of the foundations [18]. They also investigated the effect of cyclic soil degradation through a fatigue analysis based on the number of cycles [19]. It was found that the cyclic soil degradation index is a stress-dependent damage model. Based on their work, a generalized beam on Winkler foundation for the analysis of shallow and deep foundations that is suitable to be included in commercial finite element software was developed [20]. The model accounts for degradation effects under reversed cyclic loading. The effect of degradation proved to be an important parameter in describing the behaviour of SSI systems under seismic loading.

Furthermore, a very recent study by Ozkul et al. [21] used a well-defined degrading model in predicting inelastic displacement ratios using fuzzy logic techniques inheriting uncertainties in terms of strength reduction factor and periods of vibration. The results of the study show the accuracy in using the new fuzzy logic model in comparison to four other classical methods analyzed.

From the previous work of many researchers, this study is set to analyze soil interacting systems using the modified Clough model which accounts for degradation effects. The analysis is primarily based on comparison between the soil interacting and fixed-base foundation models.

2 Analytical Model

2.1 Modified Clough Model

The modified degrading Clough model initially developed in [22] and extended in [11] to account for degradation effects is used in the analysis. The model is defined by three branches: elastic branch, strain-hardening branch, and softening (cap) branch. Figure 1 shows the cyclic behaviour of the model in which the parallel section of the reloading cycle aims to reach the previous maximum displacement value set by the initial loading slope.

An energy-based approach is used to define four types of degradation effects, as described in the next section.

2.2 Degradation

All materials deteriorate as a function of loading over a period of time. Each inelastic excursion causes damage and the damage accumulates as the number of excursion increases, so it is important to include degradation effects in the model. A method developed by Rahnama and Krawinkler [23] for modelling the degradation effects is outlined with an eight-parameter energy approach. In this case, four types of cyclic degradation are considered: yield strength, unloading stiffness, accelerated stiffness and cap degradation respectively.

2.2.1 Yield Strength Degradation

Referring to the decrease of yield strength as a function of the loading history, the yield strength degradation is calculated using the following expression:

$$F_y^i = F_y^{i-1}(1 - \beta_{str}^i) \tag{1}$$

5

Where

F_y^i = Yield strength at the current path i

F_y^{i-1} = Yield Strength at the previous path $i-1$

β_{str}^i = A scalar parameter ranging from 0 to 1, accounting for yield strength degradation effect at current path i.

This scalar parameter is defined as follow:

$$\beta_{str}^i = \left(\frac{E_i}{E_{Capacity} - \sum_{j=1}^i E_j}\right)^{C_{str}} \tag{2}$$

E_i = Dissipated hysteretic energy in the current path i

$\sum_{j=1}^i E_j$ = Total energy dissipated in all paths up to the current one

C_{str} = Exponent defining the rate of deterioration = taken as 1 for this study

$E_{Capacity} = \gamma_{str} F_y \delta_y$ Energy dissipation capacity of the concrete column

Where F_y is the initial yield strength, δ_y the corresponding deformation, and γ_{str} is a constant that defines the rate of degradation. Once the total dissipated energy reaches the same value as the energy dissipation capacity, the element is assumed to be totally degraded [3].

Figure 2 shows the effect of yield strength degradation on the overall response of the element.

2.2.2 Unloading Stiffness Degradation

Unloading stiffness degradation is linked to the decrease of the unloading stiffness as a function of the loading history; this is calculated using the following expression:

$$K_{unl}^i = K_{unl}^{i-1}(1 - \beta_{unl}^i) \tag{3}$$

Where

K_{unl}^i = Unloading Stiffness at the current path i

β_{unl}^i = A scalar parameter ranging from 0 to 1, accounting for unloading stiffness degradation effect at current path i. These degradation parameters are different from the yield strength degradation in equations (1) and (2), where the values of C and γ are referred to as C_{unl} and γ_{unl} respectively.

Figure 3 shows the effect of the unloading stiffness degradation on the response of the element.

2.2.3 Accelerated Stiffness Degradation

Accelerated stiffness degradation is linked to the decrease of the reloading stiffness, which is a function of cumulative loading in peak-oriented models; this is calculated using following terms:

$$\delta_{tar}^i = \delta_{tar}^{i-1}(1 + \beta_{acc}^i) \tag{4}$$

Where

δ_{tar}^i is the displacement of the target point. The degradation parameters for β_{acc}^i are different from the yield strength and unloading degradation in which the values of C and γ are referred as C_{acc} and γ_{acc} respectively.

Figure 4 shows the effect of the accelerated stiffness degradation on the response.

2.2.4 Cap Degradation

Cap degradation is known as the inward movement of the onset point of softening as a result of cumulative damage. Cap degradation is calculated as follow:

$$\delta_{cap}^i = \delta_{cap}^{i-1}(1 - \beta_{cap}^i) \tag{5}$$

Where

δ_{cap}^i = Onset point of softening branch displacement

β_{cap}^i = Scalar parameter considering cap degradation

The Equation for β_{cap}^i is similar to equation (2) in which the values of C and γ are referred as C_{cap} and γ_{cap} respectively.

Figure 5 shows the effect of the cap degradation on the response.

2.3 Degradation effects on SDOF Systems

Figures 6-9 represent the effect of degradation on SDOF systems, ranging from zero, low, moderate and severe degradation. It is evident from the graph of the case of no degradation that the cyclic loading follows a clearly defined monotonic envelope in which the system does not experience collapse. However, for systems with degradation, the envelope of the cycle is degraded and the system can potentially experience collapse.

2.4 Collapse of Structural Elements

The elements of a structure are assumed to collapse if any of the following two criteria occur:

- Cap Failure: Displacement exceeds the intersection value of the softening (cap) slope and the residual strength.
- Cyclic Degradation Failure: the scalar parameter (β) exceeds a value of 1, in any of the different types of degradation models.

The two collapse types are represented in Figure 10.

3 Soil-Structure Interaction of SDOF System

3.1 Fixed-Base Model

A simplified model of a fixed-based foundation is shown in Figure 11. It represents multi-storey buildings with fixed-base conditions, defined with a mass (m), height (h), initial stiffness (k) and foundation circular radius (r). This equivalent system corresponds to an SDOF system with a natural period (T) and damping ratio (β) for the first mode of the structure:

$$T = 2\pi(m/k)^{0.5} \tag{6}$$

$$\beta = \frac{c}{2}(km)^{0.5} \tag{7}$$

The results from this model are used as a reference point in comparison to the soil foundation model described next.

3.2 Soil Foundation Model

In order to investigate the effect of SSI, flexible foundations with different soil properties are modelled. As shown in Figure 12, a simple spring-dashpot-mass model concept adopted from Wolf's [24] study is used to simulate the effect of SSI. The soil-structure model is based on the concept of Cone Models for foundations on the surface of homogenous half-space soil.

The SDOF system is modelled on a foundation layer with a circular disk of radius, (r). The soil beneath the foundation is characterised with soil parameters such as shear wave velocity, (V_s), dilatational wave velocity, (V_p), mass density, (ρ), and Poisson's ratio, (v).

The spring stiffness's (K_x and K_θ) and damping coefficients (C_x and C_θ) are used for the sway and rocking motions of the soil-structure model [14]. To ensure accuracy in the study, relatively accurate soil parameters are gathered from different sources outlined further in the paper.

Table 1 presents expressions for the stiffness and damping coefficients of the horizontal and torsional cones deforming in shear defined as (K_x, C_x) respectively. In addition, the stiffness and damping coefficient of the vertical and rocking cones deforming axially defined as (K_θ, C_θ) respectively are also shown in the Table.

From this the dilatational wave velocity, V_p is calculated by rearranging the equations represented by Wolf in [24]:

$$V_p = V_s . \sqrt{\frac{1-v}{1-2.v}} \tag{12}$$

Equation (12) is based on the Truncated Cone Model [25], to be used in the equivalent fixed-base model. To investigate the soil-structure interaction more accurately, the stiffness and

damping coefficients are used to derive the effective periods and damping of the soil-interacting system following the current (NEHRP) US codes [26].

3.3 Equivalent Fixed-Base Model

The effect of soil-structure interaction (SSI) is analysed by considering the effective period, $\widetilde{T}$ and effective damping, $\tilde{\beta}$, of the SDOF replacement oscillator system. Veletsos and his co-workers [4] were one of the first researchers to study the replacement oscillator [15]. The effective period and damping of the system is outline with this method in the FEMA report [26].

The effective period of the system with soil-structure interaction is as follows:

$$\widetilde{T} = T \sqrt{1 + \frac{k}{K_x}\left(1 + \frac{K_x h^2}{K_\theta}\right)} \tag{13}$$

The effective damping of the system with soil-structure interaction:

$$\tilde{\beta} = \beta_o + \frac{0.05}{\left(\frac{\tilde{T}}{T}\right)^3} \tag{14}$$

Where the β_o denotes the foundation-damping factor as mentioned in the current US codes [26].

3.4 Analysis Methodology

To compute a constant relative strength for the fixed-base model, specific strength reduction factors and inelastic displacement ratios are calculated by using dynamic time history analysis. The inelastic displacement ratio of an SDOF system with soil-structure interaction (SSI) is similar to the fixed-base model in terms of constant yield strength [15]; this simplifies the analysis without having to conduct any further iterations.

The analysis is conducted on SDOF structures with a period range of 0.2-1.4s for eight values of strength reduction factors ($R = $ 1.5, 2, 3, 4, 5, 6, 7, 8). Overall 300 different earthquake records are investigated for the fixed and flexible foundation model.

4. Data Collection and Model Validation

In this study a total of 300 earthquake records were collected from three-ground motion database; the data collection was carried out in [3] and was used for this project to increase statistical significance. To analyse the SDOF system, the earthquake data was scaled similar to [3] in order to ensure a constant hazard level in the analysis. Using the PEER Report 2007/03 in [2], five reinforced concrete columns were selected amongst 255 tested beam-columns with typical element model parameters such as the hardening slope, cap slope and cyclic deterioration. Relative soil properties corresponding to the NEHRP soil classification in [26] such as the density, shear wave velocity and shear modulus of each soil type is collected for investigation.

4.1 Earthquake Data

The 300 earthquake records used in this study were collected from the Kyoshin Network (K-Net), GeoNet and with the majority of the records, 266, from the PEER ground motion database. The earthquake motions correspond to soil type C and D according to the NEHRP soil classification in [26]. The peak ground acceleration (PGA) values of the earthquake records vary from 0.08g to 2.73g. Table 2 is a representation of the NEHRP site classification mentioned earlier; in comparison to this a similar finding by Borcherdt's [27] is shown in Table 3. Borcherdt's method of site classification is a well-known study that is also adopted by Woolery [28]. However, since the classification method is similar in both cases, the NEHRP soil classification is chosen for this study because of its simplicity.

4.2 Scaling of Earthquake Data

To evaluate the seismic performance of the SDOF system it is important to scale the earthquake records to a similar hazard level. Huang et al. [29] introduced four different scaling methods; the first method is the Geometric Mean scaling, known as amplitude scaling; however this was a complicated procedure to select ground motions with median spectrums that match closely the target spectrum of a wide range of periods [21]. The second method is the Spectrum-Matching scaling, used in nonlinear SDOF systems. The

disadvantage of this method is that for highly nonlinear SDOF systems the median peak displacement demand is underestimated [29]. The third approach is the Sa (T_1) scaling, introduced by Shome et al. [30], where the earthquake records are scaled to a specific spectral acceleration at each period of the structures vibration. Unbiased median displacement response is estimated from the results of this method [21]. The fourth method is the Distribution-Scaling, in which the median displacement responses are calculated; this method also showed no bias median displacement response predictions.

For this study, the Sa (T_1) scaling method is chosen because of its efficiency and simplicity in calculating the data for the analysis [3].

5 Numerical Results

A group of tested columns from the PEER Database [2] with similar beam-column element parameters such as hardening slope, cap slope and cyclic deterioration parameters is used in the numerical study. As an example, the corresponding force-displacement history of a selected column specimen shows a good correlation with the analytical model as shown in Figure 13.

Using the model parameters and generating 40 different periods of vibration ranging from 0.2s to 1.4s, inelastic displacement ratios for systems with fixed base and considering SSI are established. In total seven to nine different axial load values were applied on the RC columns ranging from 5% to 30% of their axial loading capacities to generate the required period values [21]. The selected RC columns are: column B2 tested by Thomsen and Wallace [31], columns C2-3 and C3-2 tested by Mo and Wang [32], column BG-6 tested by Saatcioglu and Grira [33], and column 1006015 tested by Legeron and Paultre [34]. The corresponding periods of vibration of these representative columns is shown in Figure 14.

Similar to Ozkul's [3] study, after scaling the 300 earthquake records the modified Clough model was used in order to conduct the analysis on the SDOF systems. The model parameters ensured that the analysis was based on moderately degraded SDOF systems. Assuming moderate degradation parameters, the degradation constant, $\gamma = 100$, hardening slope $\alpha_s = 6\%$, and cap slope $\alpha_c = -6\%$. Considering eight different strength reduction

12

factors ($R = 1.5, 2, 3, 4, 5, 6, 7$ and 8) with aspect ratio ($h/r = 1, 2, 3, 4$ and 5); h being the equivalent height of the element and r the foundation characteristic radius length, the maximum inelastic displacements were estimated for the SDOF system.

The aspect ratios ($h/r = 1, 2, 3, 4$ and 5) are used to calculate the equivalent period and damping of the SSI system using Equations (13-14) for different soil properties. The stiffness and rocking coefficients are shown in Tables 4-8, and the corresponding effective periods of vibration and damping ratios are shown in Tables 9 and 10 respectively. For the calculations, Poisson's ratio is assumed to equal $v = 1/3$, and the characteristic radius length of foundation is assumed to be $r = 2\,\mathrm{m}$ in the model; this is simply to analyse a typical foundation of a structure.

The soil cases for the analysis in this study were selected to represent soil C and D conditions. The three soil cases selected are:

Soil C with shear wave velocity of 360 m/s for $h/r = 1$

Soil C with shear wave velocity of 360 m/s for $h/r = 3$

Soil D with shear wave velocity of 180 m/s for $h/r = 5$.

5.1 Displacement Estimates of RC Columns

In general, there is a period shift for the SSI systems considered; however, the change in effective periods was more evident in cases where the structure is more slender (aspect ratio $h/r = 5$) and softer soil conditions (soil D). Moreover, it is evident from the calculations that the change in period is very small for all soil cases with aspect ratio $h/r = 1$ in comparison to the fixed-base condition.

Other factors such as the effective damping ratio when considering soil foundation are likely to affect the inelastic displacement ratios. The effective damping ratios show a relative difference for each soil case when compared to the fixed-base foundation. Particularly for soil type D, whereby the period lengthening ratio ($\tilde{T}/T$) is sufficiently large to increase the damping values compared to soil C where this lengthening ratio was small enough to neglect the β_o factor in the analysis.

Furthermore, collapse of the system was defined when more than 50% of the 300 earthquake records failed; this probabilistic approach is similar to the work in [3] and [21]. The collapse point was identified with a " * " on the graph, and the collapse periods for different strength reduction factors are shown in Table (11).

The results of the inelastic displacement ratios are presented in Figures 15-22.

5.2 Discussion of Results

From the inelastic displacement ratio (IDR) calculated for the different strength reduction factors ($R = 1.5$, 2, 3, 4, 5, 6, 7 and 8) as shown in Figures 15-22, it is evident that the IDR values generally decrease as the period increases for the system. However, this is not always valid, as for strength reduction factors greater than $R = 2$, the IDR values fluctuate for periods less than 0.6 seconds, these results are similar to [3].

Figures 15-16 for strength reduction factors $R = 1.5$ and 2 respectively, do not depict a major difference in the inelastic displacement ratios for the cases of fixed-base and SSI conditions; however as the system starts to yield and degradation takes effect, the difference between the fixed and flexible foundation becomes clearer. Furthermore, the IDR values after a period of 0.6 seconds somewhat follow the equal displacement rule (i.e. maximum inelastic displacement approximately equal to maximum elastic) for all cases considered.

It is evident from the graphs, particularly for strength reduction factors, $R > 3$, that the inelastic displacement ratios for soil type C and D have generally lower values in comparison to the fixed-base IDR values; however, this does not justify whether or not the maximum inelastic deformation of the system is greater for the soil foundation when compared to the fixed-base foundation model. For example, the calculated inelastic displacement for a system with $R = 3$ at 0.197s period show that for soil case D and $h/r = 5$ the inelastic deformation is greater when compared with other soil types and the fixed-base foundation. Although the IDR value for the fixed-base is higher, the elastic displacement of the system is lower than for the case of soil type D, and the resulting fixed-base inelastic displacement is

14

also lower. In general, the inelastic displacement is found to be higher as the soil conditions become softer and as the aspect ratio increases.

These results show a great significance in including the SSI effect in earthquake design of SDOF structures, particularly for soft soil D and when the aspect ratio is high (e.g. $h/r = 5$). For periods less than 0.6s, the aspect periods has a major effect on the IDR value of a system; however, for periods greater than 0.6s the IDR values approximately equal to one, satisfying the equal displacement rule.

6. Mathematical Expressions for Inelastic Ratios of Degrading SSI Systems

The results obtained in the study were used to develop approximate equations for the assessment of inelastic displacement ratios of degrading SDOF systems. Using the equation originally proposed by Nassar and Krawinkler in [8], a modified expression is proposed for the degrading modified Clough SSI models:

$$c = \frac{T^a}{1 + T^a} + \frac{b}{T} \tag{15}$$

$$\frac{\delta_{inelastic}}{\delta_{elastic}} = \frac{1}{R}\left[1 + \frac{R^c - 1}{c}\right] \tag{16}$$

Using a least square fit procedure, the coefficient values of a and b were recalibrated for the degrading SSI system. The proposed values are:

$$a = \tilde{T}/T - 0.46 \text{ and } b = 1.42 - \left(\sqrt{\tilde{T}/T}\right) - \frac{R}{50} + \frac{0.033R^2}{\sqrt{\gamma}} \tag{17}$$

where γ is the degradation parameter, $R=$ strength reduction factor; $T=$ fundamental period of the structure, $\tilde{T}=$ effective period of the SSI system which is a function of *h/r*.

The results shown in Figures 23-26 suggest that there is a good agreement between the mathematical equation and numerical results. Specifically, the inelastic displacement ratios

using the mathematical equation are showing slightly higher values in all cases in comparison to the model results, suggesting a conservative approach for design purposes. Overall, the benefits of this mathematical function are that it can estimate maximum inelastic displacements of RC structures with varying aspect ratio of the foundation, different strength reduction factors, and for any given period under seismic forces.

7 Conclusions

In this study, the soil-structure interaction is investigated for SDOF systems for a period range of 0.2-1.4s using the modified degrading Clough model. The behaviour of RC columns subjected to 300 different earthquake motions recorded on firm soil conditions is analysed through 384,000 dynamic analyses. With the effective period and effective damping values differing from the fixed-base case, the maximum inelastic displacement response of the system is established for the soil interacting system. From the results of this study the following conclusions can be drawn:

1. The effect of soil-structure interaction for soil type C with aspect ratio, $h/r = 1$ & 3 are negligible, whereas for soil type D and $h/r = 5$, it should be considered in the performance-based earthquake design process. Particularly for short period region, the inelastic displacement ratios (IDR) for the interacting and fixed-base systems are considerably different.

2. Soil types C & D show lower IDR values than the fixed-base case. The difference was clearer for soil type D, in comparison to soil type C and the fixed-base case.

3. From the results, higher IDR values do not represent the most critical case; however, when the maximum inelastic displacement of the system was calculated, it showed that soil type D was the most critical case as the inelastic displacements were higher than soil type C and the fixed-base case. Particularly for the softer soil type D with properties such as lower values of shear wave velocity, mass density and shear

16

modulus in comparison to soil type C, the effect of soil-structure interaction was more noticeable.

4. The aspect ratio (h/r) used in the study is an important parameter that affect the value of IDR. From the results, there is a decrease in IDR values for $h/r = 5$ in comparison to other cases where $h/r = 1$ & 3 to a period of around 0.6s, but for periods higher than 0.6s, the effect of aspect ratios on IDR values is negligible as these values approximately equal to one satisfying the equal displacement rule. Therefore, for periods less than 0.6s, the effect of soil-structure interaction should be considered in the seismic design for systems with higher aspect ratios.

5. The proposed mathematical expression originally developed in [8] and recalibrated for the case of SSI provides good estimate for the inelastic displacement ratios of soil interacting systems.

REFERENCES

[1] Pacific Earthquake Engineering Research Center (PEER). (2014, June) PEER structural performance database. [Online].   HYPERLINK "http://nisee.berkeley.edu/spd/search.html" http://nisee.berkeley.edu/spd/search.html

[2] C. B. Haselton, A. B. Liel, S. T. Lange, and G. G. Deierlein, "Beam–column element model calibrated for predicting flexural response leading to global collapse of RC framing buildings," Pacific Earthquake Engineering Research Center, University of California, Berkeley, PEER Report 2007/03, 2008.

[3] S. Ozkul, "New inelastic displacement ratio of SDOF structures using expert systems," University of Houston, Master Thesis 2011.

[4] A. S. Veletsos and N. M. Newmark, "Effect of inelastic behavior on the response of simple systems to earthquake motions," in Proceedings of the Third World Conference on Earthquake Engineering, Japan, 1960, pp. 895-912.

[5] K. Shimazaki and M. A. Sozen, "Seismic drift of reinforced concrete structures," Technical Research Reports of Hazama-Gumi Ltd, Tokyo, 1984.

[6] E. Miranda, "Inelastic displacement ratios for structures on firm sites," Journal of Structural Engineering, vol. 126, no. 10, pp. 1150-1159, October 2000.

[7] J. Ruiz-Garcia and E. Miranda, "Inelastic displacement ratios for evaluation of existing structures," Earthquake Engineering & Structural Dynamics, vol. 32, no. 8, pp. 1237-1258, July 2003.

[8] A.A. Nassar and H. Krawinkler, "Seismic demands for SDOF and MDOF systems," Stanford University, Stanford, Report No. 95, 1991.

[9] A. M. Halabian and M. Hesham El Naggar, "Effects of non-linear soil-structure interaction on seismic response of tall slender structures," Soil Dynamics and Earthquake Engineering, vol. 22, no. 8, pp. 639-658, September 2002.

[10] A. K. Chopra and C. Chintanapakdee, "Inelastic deformation ratios for design and evaluation of structures: Single-degree-of-freedom bilinear systems," Journal of Structural Engineering, vol. 130, no. 9, pp. 1309-1319, September 2004.

[11] M. Chenouda and A. S. Ayoub, "Inelastic displacement ratios of degrading systems," Journal of Structural Engineering, vol. 134, no. 6, pp. 1030-1045, June 2008.

[12] M. Chenouda and A. S. Ayoub, "Probabilistic collapse analysis of degrading Multi Degree of Freedom structures under earthquake excitation," Engineering Structures, vol. 31, no. 12, pp. 2909-2921, September 2009.

[13] A. S. Ayoub and M. Chenouda, "Response spectra of degrading structural systems," Engineering Structures, vol. 31, no. 7, pp. 1393-1402, July 2006.

[14] M. Eser, C. Aydemir, and I. Ekiz, "Inelastic displacement ratios for structures with foundation flexibility," KSCE Journal of Civil Engineering, vol. 16, no. 1, pp. DOI: 10.1007/s12205-012-1266-5, January 2012.

[15] M. Aydemir, "Inelastic displacement ratios for evaluation of stiffness degrading structures with soil structure interaction built on soft soil sites," Structural Engineering and Mechanics, vol. 45, no. 6, pp. 741-758, February 2013.

[16] F. Khoshnoudian, E. Ahmadi, and F. A. Nik, "Inelastic displacement ratios for soil-structure systems," Engineering Structures, vol. 57, pp. 453-464, December 2013.

[17] N. Allotey and M. Hesham El Naggar, "Analytical moment–rotation curves for rigid foundations based on a Winkler model," Soil Dynamics and Earthquake Engineering, vol. 23, no 5, pp. 367–381, July 2003.

[18] H. El Ganainy and M.H. El Naggar, "Efficient 3D nonlinear Winkler model for shallow foundations," Soil Dynamics and Earthquake Engineering, vol. 29, no. 8, pp. 1236-1248, August 2009.

[19] N. Allotey and M. Hesham El Naggar, "A Consistent Soil Fatigue Framework Based on the Number of Equivalent Cycles," Geotechnical and Geological Engineering, vol. 26, no. 1, pp. 65-77, August 2007.

[20] N. Allotey and M. Hesham El Naggar, "Generalized dynamic Winkler model for nonlinear soil–structure interaction analysis," Canadian Geotechnical Journal, vol. 45, no. 4, pp. 560-573, May 2008.

[21] S. Ozkul, A. S. Ayoub, and A. Altunkaynak, "Fuzzy-logic based inelastic displacement ratios of degrading RC structures," Engineering Structures, vol. 75, pp. 590-603, September 2014.

[22] R.W. Clough and S.B. Johnston, "Effect of stiffness degradation on earthquake ductility requirements," in 2nd Japan Earthquake Engineering Symposium, 1966, pp. 195-198.

[23] M. Rahnama and H. Krawinkler, "Effects of soils and hysteresis models on seismic design spectra," The John A. Blume Earthquake Engineering Center, Stanford University, Stanford, Report 117, 1993.

[24] John P. Wolf, Foundation vibration analysis using simple physical models. NJ: Prentice-Hall, 1994, p. 423.

[25] J. W. Meek and J. P. Wolf, "Cone models for homogeneous soil," Journal of Geotechnical Engineering, vol. 118, no. 5, pp. 667-685, 1992.

[26] Federal Emergency Management Agency (FEMA), "NEHRP recommended provisions for seismic regulations for new buildings and other structures," FEMA-450, 2003.

[27] R. D. Borcherdt, "An integrated methodology for estimates of site-dependent response spectra, seismic coefficients for site dependent building code provisions, and predictive GIS maps of strong ground shaking," in New Developments in Earthquake Ground Motion Estimation and Implications for Engineering Design Practice, 1994, pp. 10-44.

[28] E. Woolery, R. Street, Z. Wang, and I. E. Harik, "Soil classifications for estimating site-dependent response spectra and seismic coefficients for building code provisions in western Kentucky," Engineering Geology, vol. 46, no. 3-4, pp. 331-347, July 1997.

[29] Y. N. Huang, A. S. Whittaker, N. Luco, and R. O. Hamburger, "Scaling earthquake ground motions for performance-based assessment of buildings," J. Struct. Eng., vol. 137, no. 3, pp. 311-321, March 2011.

[30] N. Shome, C. A. Cornell, P. Bazurro, and J. E. Carballo, "Earthquakes, records, and nonlinear reponses," Earthquake Spectra, vol. 14, no. 3, pp. 469-500, August 1998.

[31] J. H. Thomsen and J. W. Wallace, "Lateral load behavior of reinforced concrete columns constructed using high-strength materials," ACI Structural Journal, vol. 91, no. 5, pp. 605-615, September 1994.

[32] Y. L. Mo and S. J. Wang, "Seismic Behavior of RC Columns with Various Tie Configurations," Journal of Structural Engineering, vol. 126, no. 10, pp. 1122-1130, October 2000.

[33] M. Saatcioglu and M. Grira, "Confinement of reinforced concrete columns with welded reinforcement grids," ACI Structural Journal, vol. 96, no. 1, pp. 29-39, January 1999.

[34] F. Legeron and P. Paultre, "Behavior of high-strength concrete columns under cyclic flexure and constant axial load," ACI Structural Journal, vol. 97, no. 4, pp. 591-601, January 2000.

Table 1 Stiffness and damping coefficients of Cone Model [20]

Horizontal Stiffness Coefficient:	$$K_x = \frac{8.\rho.V_s^2.r}{2-v}$$	(8)
Vertical Stiffness Coefficient:	$$K_\theta = \frac{8.\rho.V_s^2.r^3}{3.(1-v)}$$	(9)
Horizontal Damping Coefficient:	$$C_x = \rho.V_s.\pi.r^2$$	(10)
Rocking Damping Coefficient:	$$C_\theta = \rho.V_p.\pi.\frac{r^4}{4}$$	(11)

Table 2 FEMA 450 NEHRP Site Classification in [22]

Site Class	Soil Profile Name	Shear-Wave Velocity V_s in Top 100 ft (30m)	
		(Ft/s)	(m/s)
A	Hard Rock	$V_s > 5000$	$V_s > 1500$
B	Rock	$2500 < V_s \leq 5000$	$760 < V_s \leq 1500$
C	Very Dense Soil and Soft Rock	$1200 < V_s \leq 2500$	$360 < V_s \leq 760$
D	Stiff Soil Profile	$600 < V_s \leq 1200$	$180 < V_s \leq 360$
E	Soft Soil Profile	$V_s < 600$	$V_s < 180$

Table 3 Borcherdt's Site Classification Method in [25]

Borcherdt's Method			Comparison to NEHRP Site Class
Site Class	**Soil Profile Name**	**Shear-Wave Velocity, V_s (m/s)**	
SC-I	Firm and Hard Rocks		A
SC-Ia	Hard Rocks	1620	
SC-Ib	Firm to Hard Rocks	1050	B
SC-II	Gravelly Soils and Soft to Firm Rocks	540	C
SCIII	Stiff Clays and Sandy Soils	290	D
SC-IVa	Soft Soils	150	E
SC-IVb	Non-Special-Study Soft Soils		

Table 4 Stiffness and rocking coefficients of RC Columns for $r = 1$m foundation

Soil Type	K_x (kN/m)	K_θ (kN/m)	C_x (kNm/s)	C_θ (kN/m s)
	6265804.8	5221504	5395.999542	2697.999771
C	3401932.8	2834944	3975.999662	1987.999831
	1405900.8	1171584	2555.999783	1277.999891
	1244160	1036800	2261.946711	1130.973355
D	699840	583200	1696.460033	848.2300165
	311040	259200	1130.973355	565.4866776

Table 5 Stiffness and rocking coefficients of RC Columns for $r = 1.5$m foundation

Soil Type	K_x (kN/m)	K_θ (kN/m)	C_x (kNm/s)	C_θ (kN/m s)
	9398707.2	17622576	12140.99897	13658.62384
C	5102899.2	9567936	8945.99924	10064.24915
	2108851.2	3954096	5750.999512	6469.874451
	1866240	3499200	5089.380099	5725.552611
D	1049760	1968300	3817.035074	4294.164458
	466560	874800	2544.690049	2862.776306

Table 6 Stiffness and rocking coefficients of RC Columns for $r = 2$m foundation

Soil Type	K_x (kN/m)	K_θ (kN/m)	C_x (kNm/s)	C_θ (kN/m s)
C	12531609.6	41772032	21583.99817	43167.99633
	6803865.6	22679552	15903.99865	31807.9973
	2811801.6	9372672	10223.99913	20447.99826
D	2488320	8294400	9047.786842	18095.57368
	1399680	4665600	6785.840132	13571.68026
	622080	2073600	4523.893421	9047.786842

Table 7 Stiffness and rocking coefficients of RC Columns for $r = 2.5$m foundation

Soil Type	K_x (kN/m)	K_θ (kN/m)	C_x (kNm/s)	C_θ (kN/m s)
C	15664512	81586000	33724.99714	105390.6161
	8504832	44296000	24849.99789	77656.24341
	3514752	18306000	15974.99864	49921.87076
D	3110400	16200000	14137.16694	44178.64669
	1749600	9112500	10602.87521	33133.98502
	777600	4050000	7068.583471	22089.32335

Table 8 Stiffness and rocking coefficients of RC Columns for $r = 3m$ foundation

Soil Type	K_x (kN/m)	K_θ (kN/m)	C_x (kNm/s)	C_θ (kN/m s)
C	18797414.4	140980608	48563.99588	218537.9814
	10205798.4	76543488	35783.99696	161027.9863
	4217702.4	31632768	23003.99805	103517.9912
D	3732480	27993600	20357.5204	91608.84178
	2099520	15746400	15268.1403	68706.63133
	933120	6998400	10178.7602	45804.42089

Table 9 Effective periods of vibration of the RC Columns

Column B2, Effective Periods (s)			
Fixed-Base	**Soil C - $h/r = 1$**	**Soil C - $h/r = 3$**	**Soil D - $h/r = 5$**
0.197423278	0.19819438	0.201524664	0.241672508
0.241793148	0.242737551	0.246816299	0.295987166
0.279198678	0.280289181	0.284998914	0.34177654
0.312153611	0.31337283	0.318638472	0.382117787
0.341947149	0.343282737	0.349050958	0.418589065
0.369345134	0.370787734	0.377018125	0.452127864
0.394846556	0.39638876	0.403049328	0.483345017
Column C2-3, Effective Periods (s)			
Fixed-Base	**Soil C - $h/r = 1$**	**Soil C - $h/r = 3$**	**Soil D - $h/r = 5$**
0.335647816	0.337651537	0.346259382	0.445628898
0.375265667	0.377505895	0.387129758	0.498228255
0.411082942	0.413536989	0.424079403	0.545781709
0.444020325	0.446670999	0.458058107	0.589511621
0.474677694	0.477511383	0.489684714	0.630214432
0.503471725	0.506477306	0.519389074	0.668443349
0.530705796	0.533873957	0.547484155	0.704601156
0.556608934	0.559931729	0.574206225	0.738991926
0.581359071	0.584829617	0.599738842	0.771851893
Column BG-6, Effective Periods (s)			
Fixed-Base	**Soil C - $h/r = 1$**	**Soil C - $h/r = 3$**	**Soil D - $h/r = 5$**
0.670473526	0.673888943	0.688594365	0.861379871
0.694006033	0.697541325	0.712762883	0.891612874
0.716766348	0.720417582	0.736138339	0.920853815
0.738825841	0.742589447	0.758794033	0.949194387
0.760245518	0.764118237	0.780792618	0.976712966
0.781078020	0.78505686	0.802188158	1.003477181
0.801369140	0.805451344	0.823027685	1.029545865
Column 1006015, Effective Periods (s)			
Fixed-Base	**Soil C - $h/r = 1$**	**Soil C - $h/r = 3$**	**Soil D - $h/r = 5$**
0.720322232	0.721730317	0.72784281	0.805102844
0.831756469	0.833382386	0.840440485	0.929652687
0.929932003	0.931749833	0.939641028	1.039383303
1.018689470	1.020680803	1.029325174	1.138587361
1.100310385	1.10246127	1.111798258	1.229814909
1.176281280	1.178580673	1.188562333	1.31472744
1.247634704	1.250073579	1.260660728	1.394479032
1.315122451	1.317693251	1.328853086	1.469909963
			0.805102844
Column C3-2, Effective Periods (s)			
Fixed-Base	**Soil C - $h/r = 1$**	**Soil C - $h/r = 3$**	**Soil D - $h/r = 5$**
0.314696529	0.316342487	0.32342684	0.406432472
0.363380251	0.36528084	0.373461146	0.469307794
0.406271472	0.408396395	0.417542255	0.524702065
0.445048099	0.447375836	0.457394623	0.574782314
0.480706888	0.483221131	0.494042658	0.620835855
0.513897280	0.516585119	0.528153818	0.663701447
0.545070377	0.54792126	0.560191719	0.703961691
0.574554626	0.577559721	0.59049392	0.742040777
0.602597975	0.605749745	0.619315248	0.778258932

Table 10 Effective Damping ratio of the RC Columns

Effective Damping Ratio, ($\widetilde{\beta}$)				
Column	**Fixed-Base**	**Soil C - $h/r = 1$**	**Soil C - $h/r = 3$**	**Soil D - $h/r = 5$**
B2	0.05	0.049418672	0.047008941	0.052257331
C2-3	0.05	0.049115129	0.045542496	0.053364928
BG-6	0.05	0.049243614	0.046155612	0.051579291
1006015	0.05	0.049707923	0.048466055	0.048809345
C3-2	0.05	0.04922359	0.046059338	0.053210295

Table 11 Collapse periods for moderately degrading SDOF RC Columns

Collapse Period (s)	$R = 1.5$	$R = 2$	$R = 3$	$R = 4$	$R = 5$	$R = 6$	$R = 7$	$R = 8$
Fixed-Base	-	-	-	0.242	0.279	0.315	0.406	0.406
Soil C $h/r = 1$	-	-	-	0.242	0.280	0.316	0.408	0.408
Soil C $h/r = 3$	-	-	-	0.247	0.285	0.323	0.417	0.417
Soil D $h/r = 5$	-	-	-	-	0.296	0.342	0.419	0.498

Table 12 Inelastic displacements for a SDOF system with $R = 3$

Period: 0.197423278s	Inelastic Displacement Ratio	Maximum Elastic Displacement (mm)	Maximum Inelastic Displacement (mm)
Fixed-base	1.976768198	0.5811	1.14869999986
Soil C $h/r = 1$	1.949718286	0.5857	1.14195000011
Soil C $h/r = 3$	1.77968621	0.6055	1.07760000016
Soil D $h/r = 5$	1.367191089	0.8708	1.1905500003
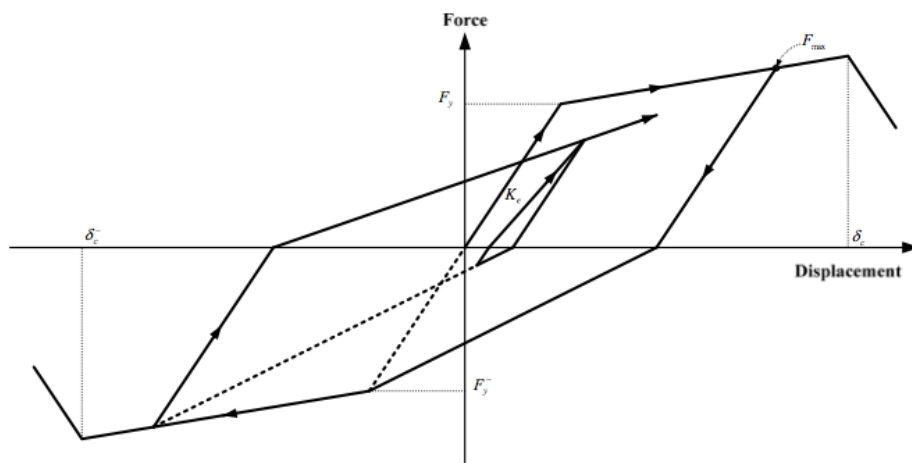
Figure 1 Modified Clough Model as represented in [13]
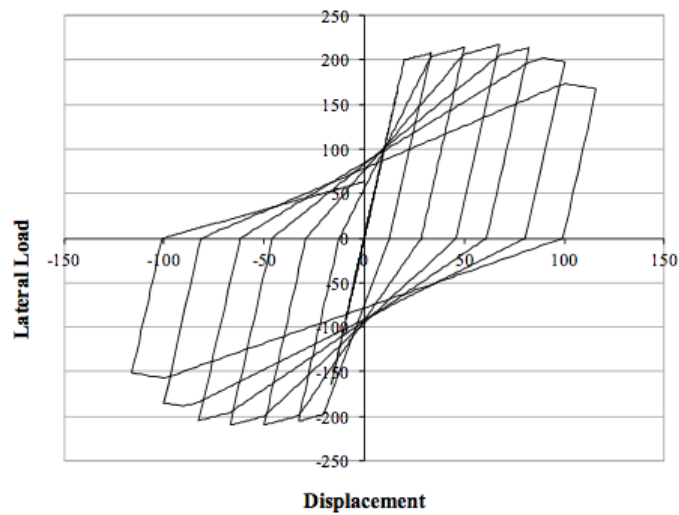
Figure 2. Yield Strength Degradation of modified Clough model in [3]
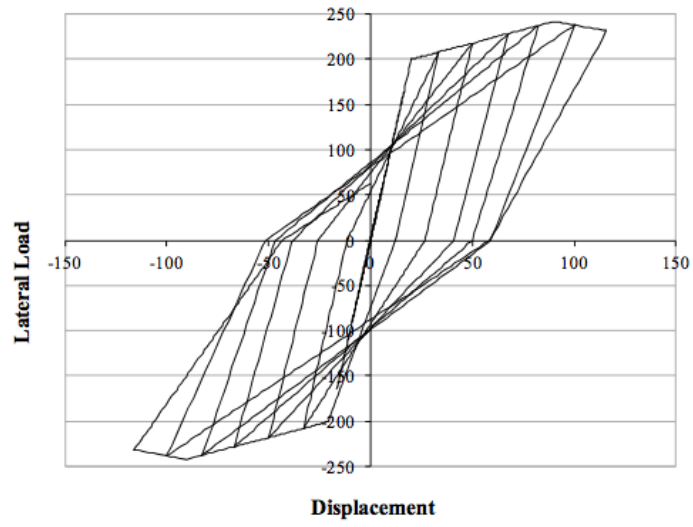
Figure 2. Unloading Stiffness Degradation of modified Clough model in [3]
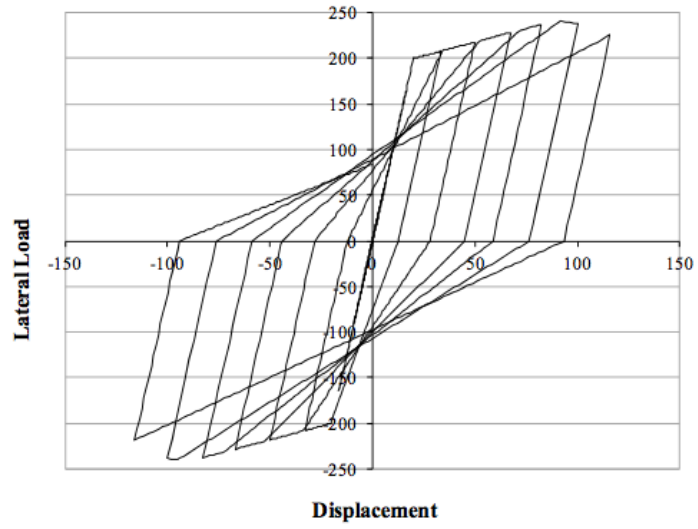
Figure 3. Accelerated Stiffness Degradation of modified Clough model in [3]
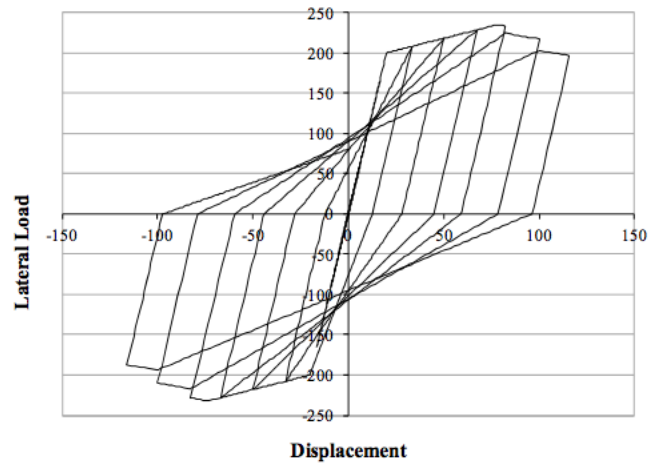
Figure 4. Cap Degradation of modified Clough model in [3]
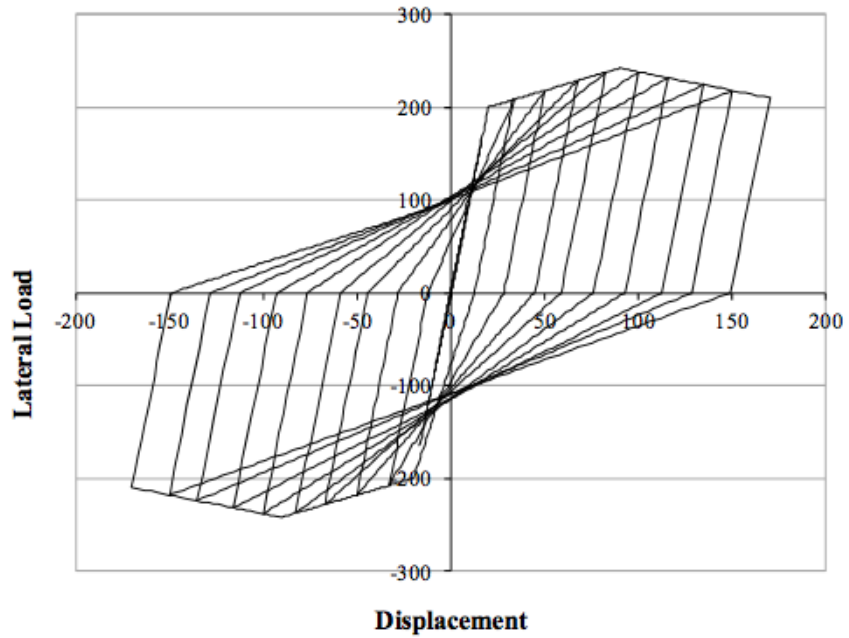
Figure 5. Model – No Degradation in [3]
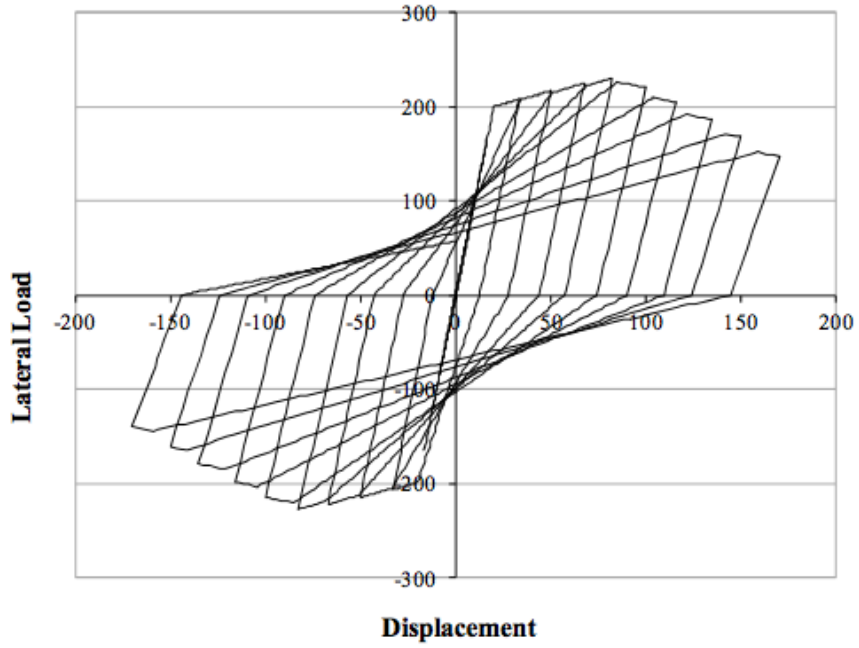
Figure 6. Model – Low Degradation in [3]
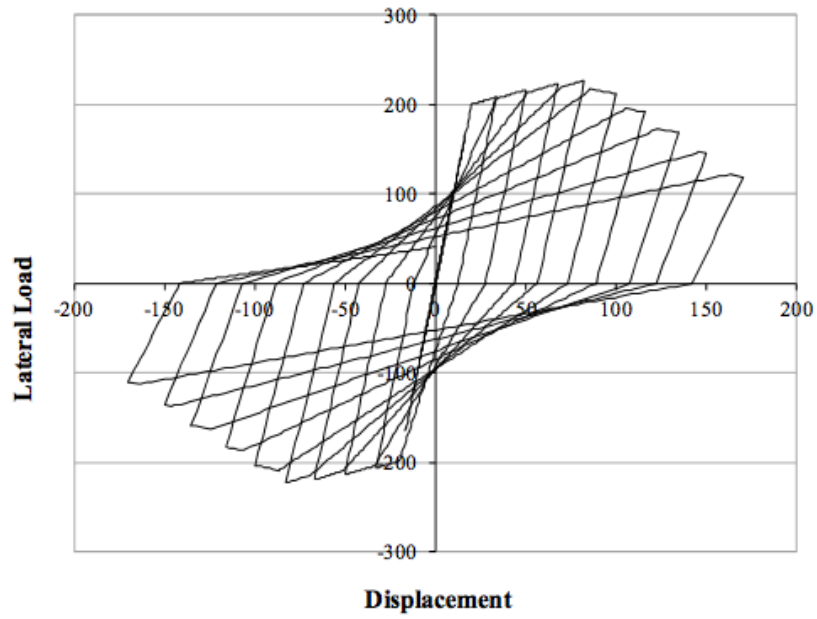
Figure 7. Model – Moderate Degradation in [3]
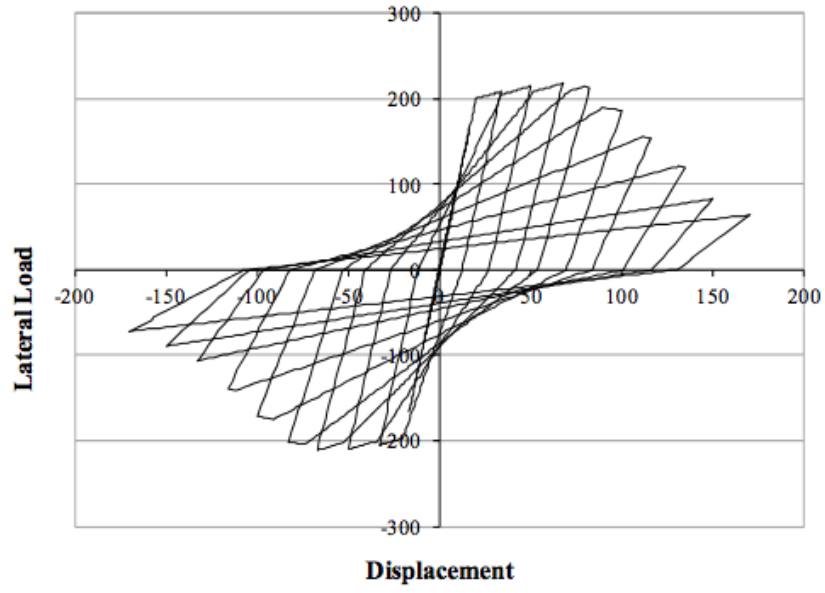
Figure 8. Model – Severe Degradation in [3]
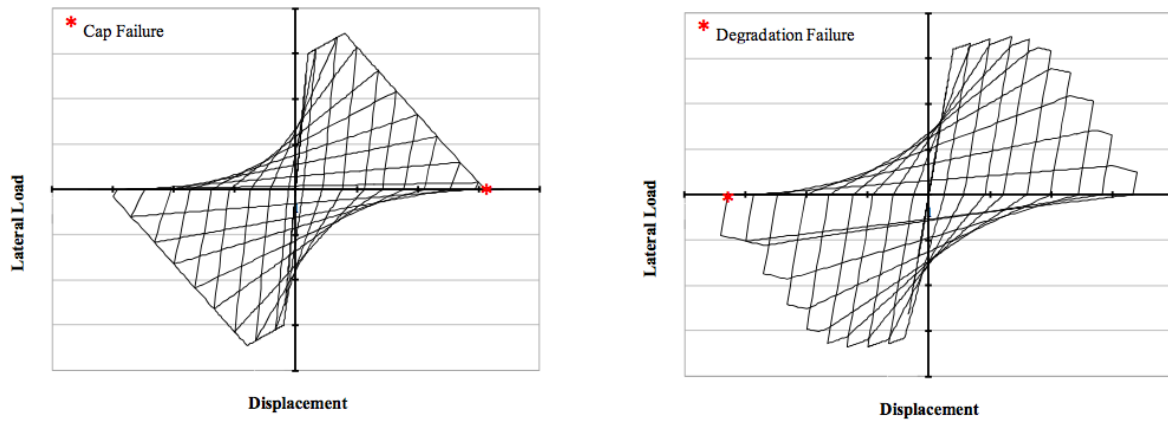
Figure 9. Collapse types: Cap and degradation failure in [3]
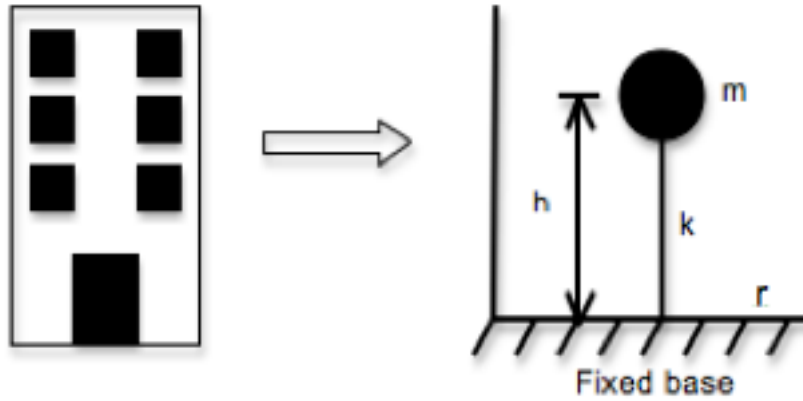
Figure 11. Soil-structure model of a fixed-based SDOF system
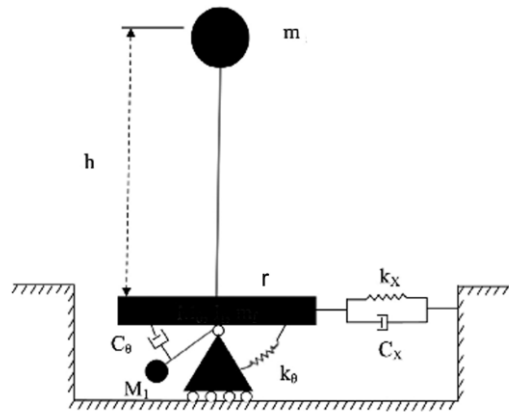
Figure. 110 Soil-structure model with soil foundation in [19]
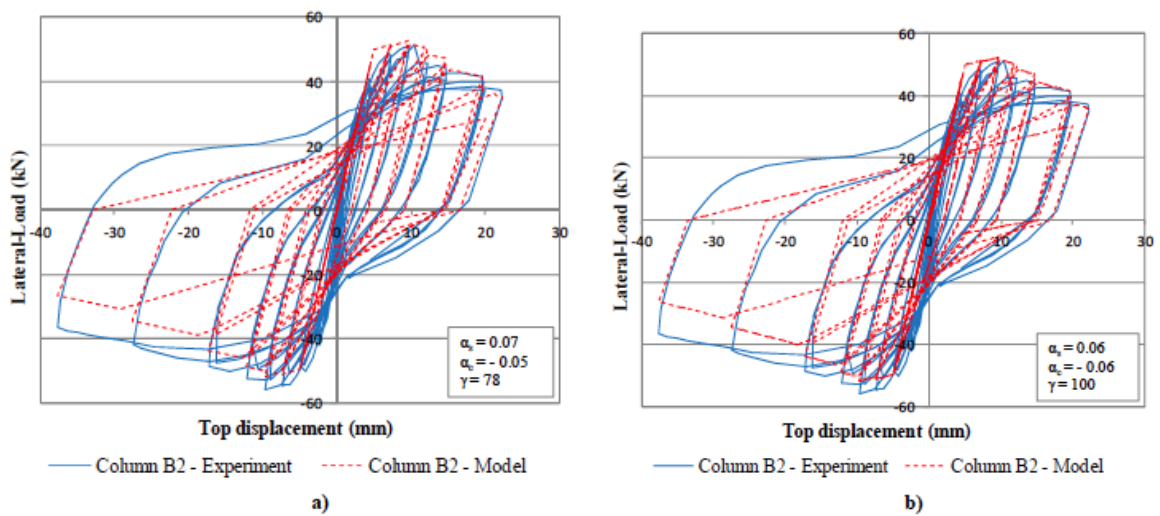
Figure. 13 Force-Displacement Response of Column B2 a) using PEER Report 2007/03 recommended beam-column element parameters b) using model parameters
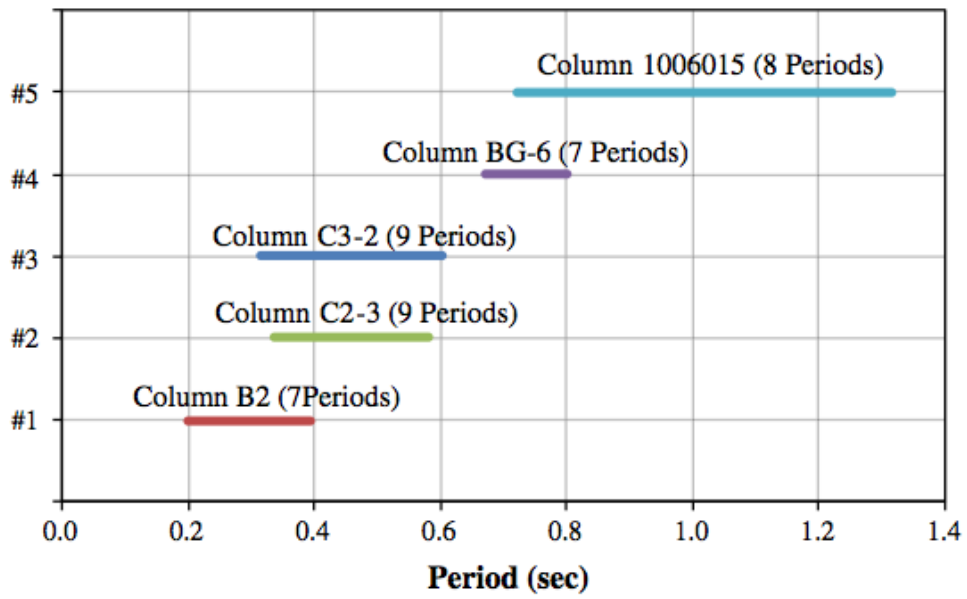
Figure. 114 Period of vibration range of each RC column selected in [21]
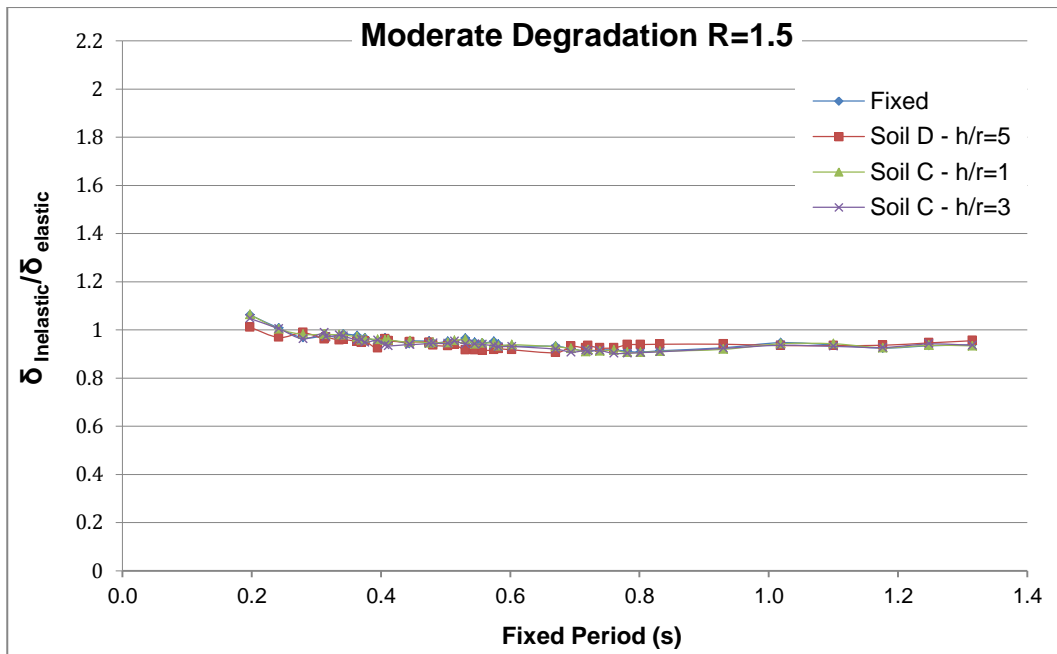
Figure. 15 Inelastic Displacement Ratio of SDOF RC Columns when R=1.5
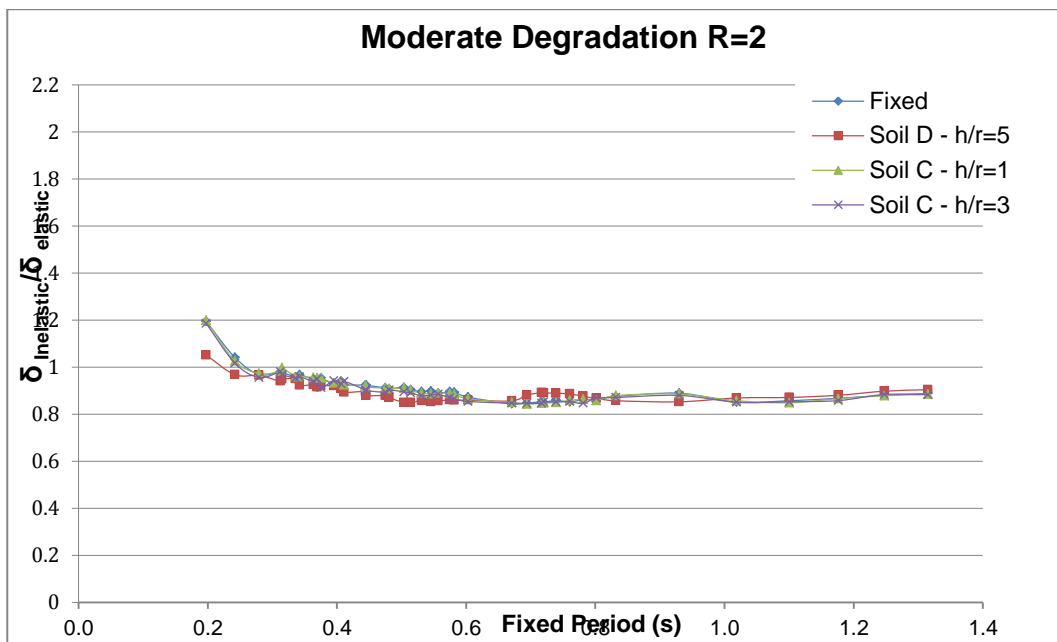
Figure. 16 Inelastic Displacement Ratio of SDOF RC Columns when R=2
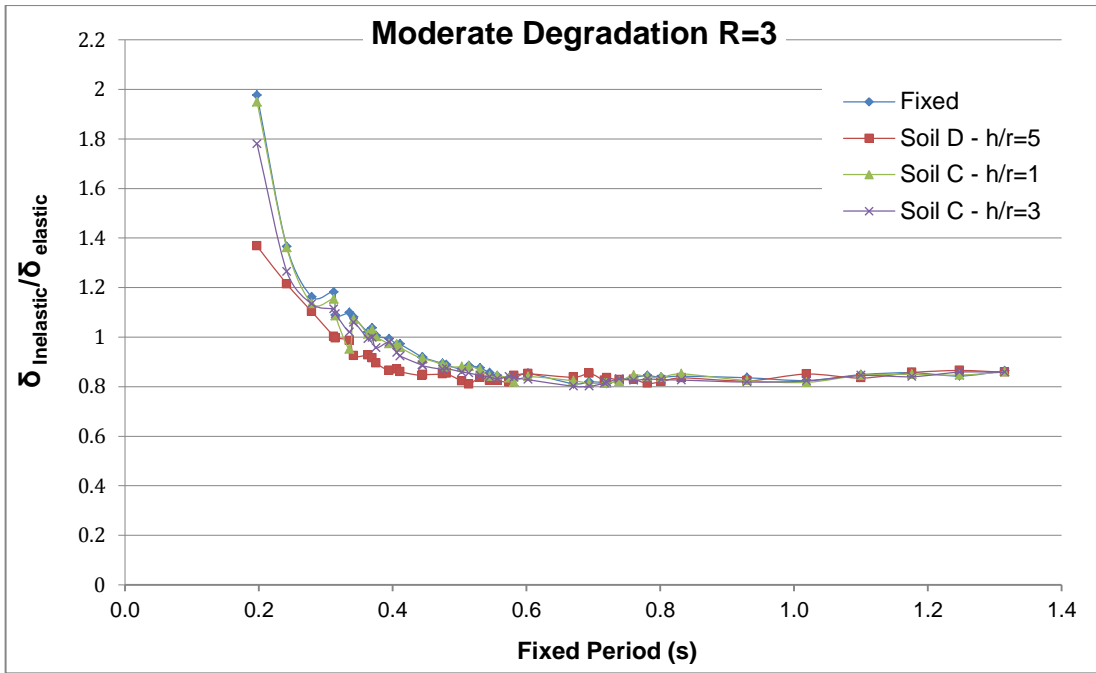
Figure. 17 Inelastic Displacement Ratio of SDOF RC Columns when R=3
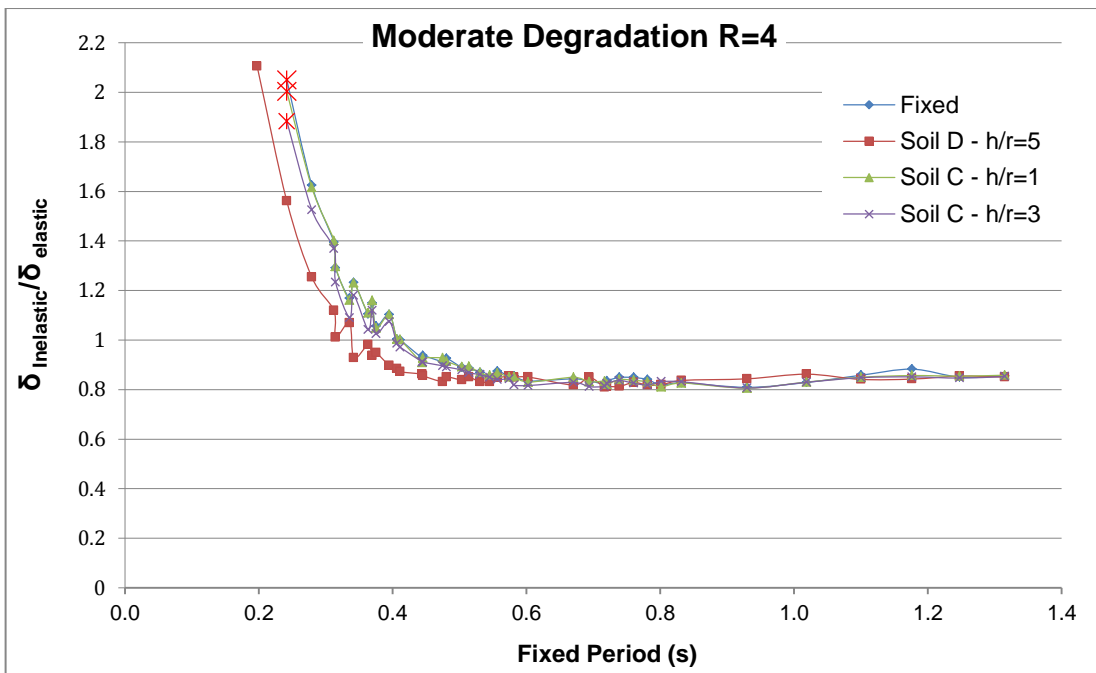
Figure. 18 Inelastic Displacement Ratio of SDOF RC Columns when R=4
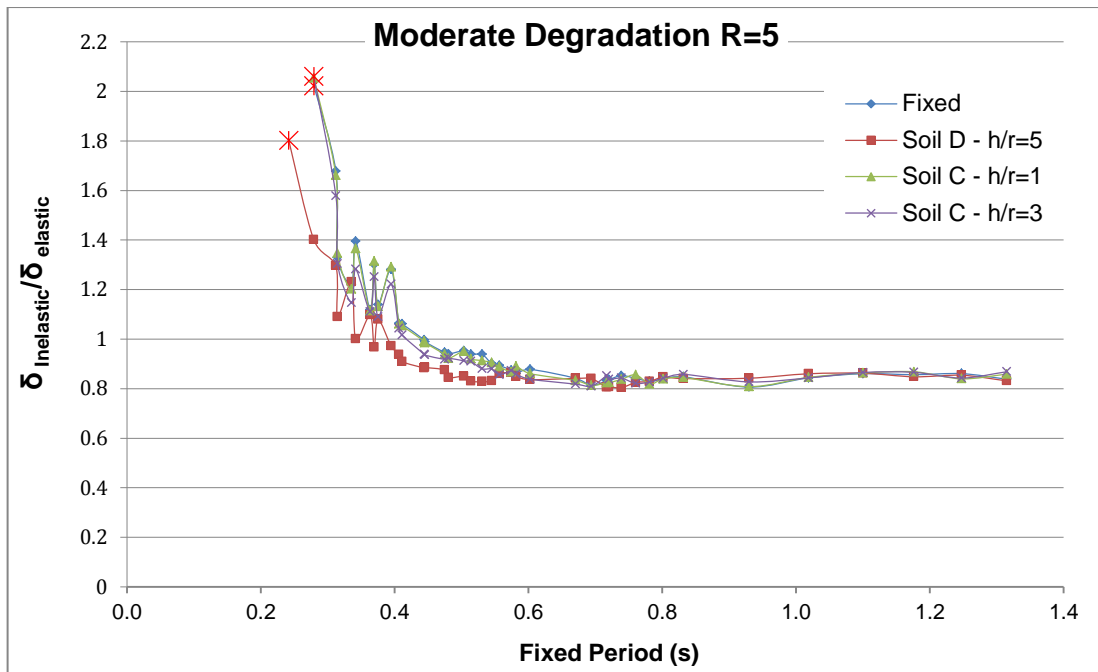
**Figure. 19** Inelastic Displacement Ratio of SDOF RC Columns when R=5
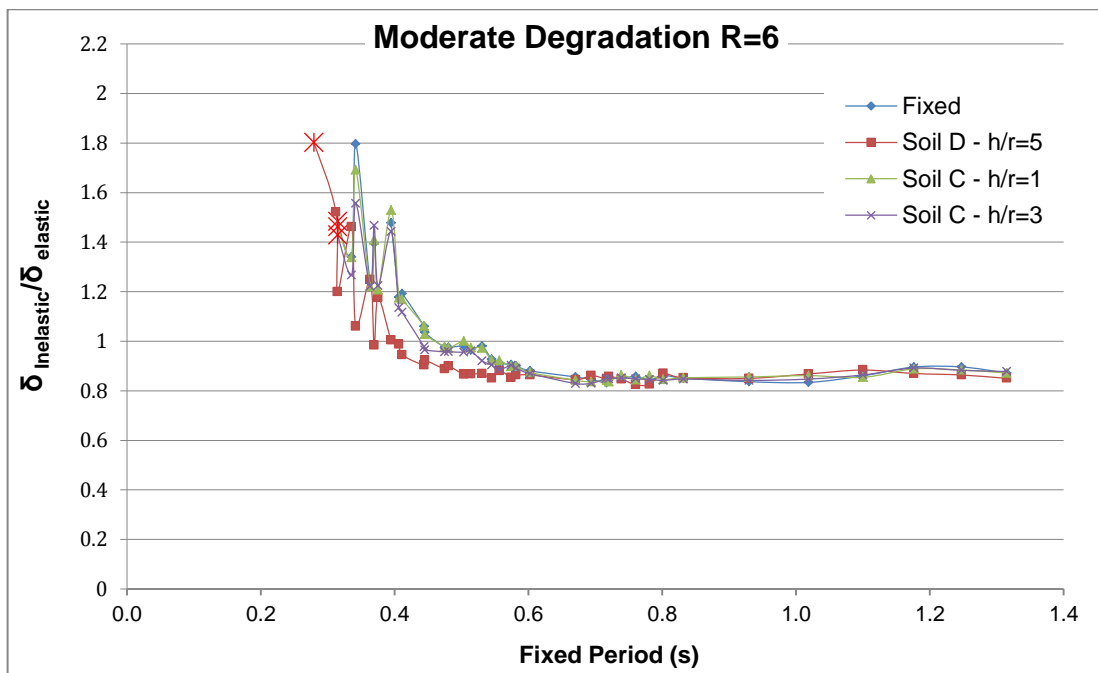
**Figure. 20** Inelastic Displacement Ratio of SDOF RC Columns when R=6
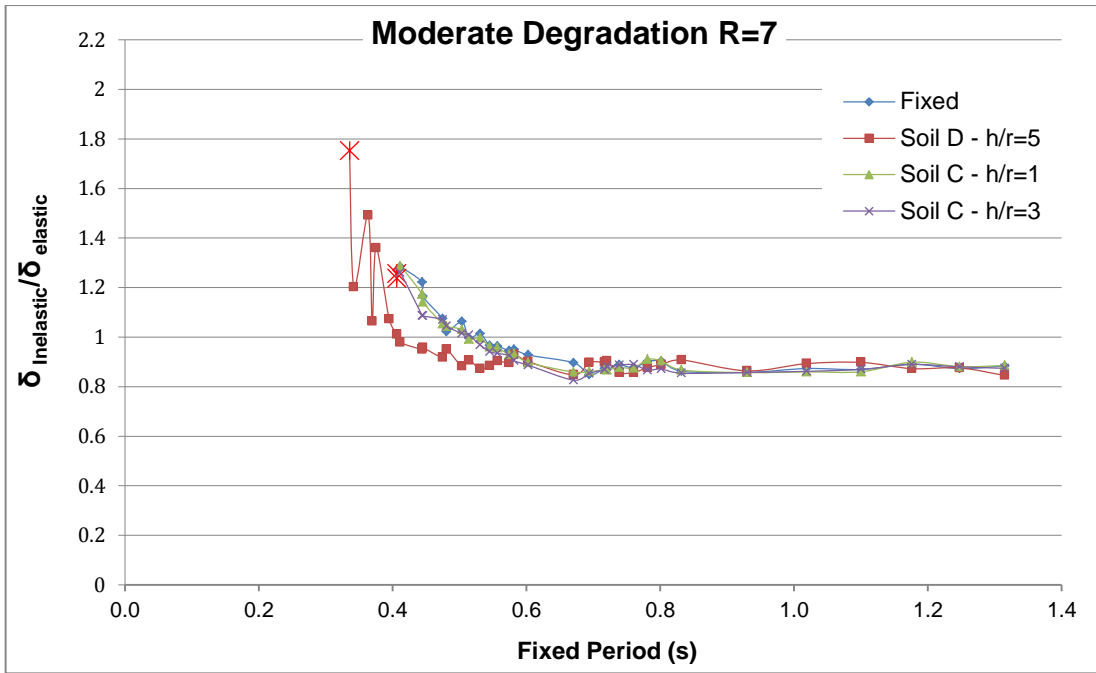
**Figure. 21** Inelastic Displacement Ratio of SDOF RC Columns when R=7
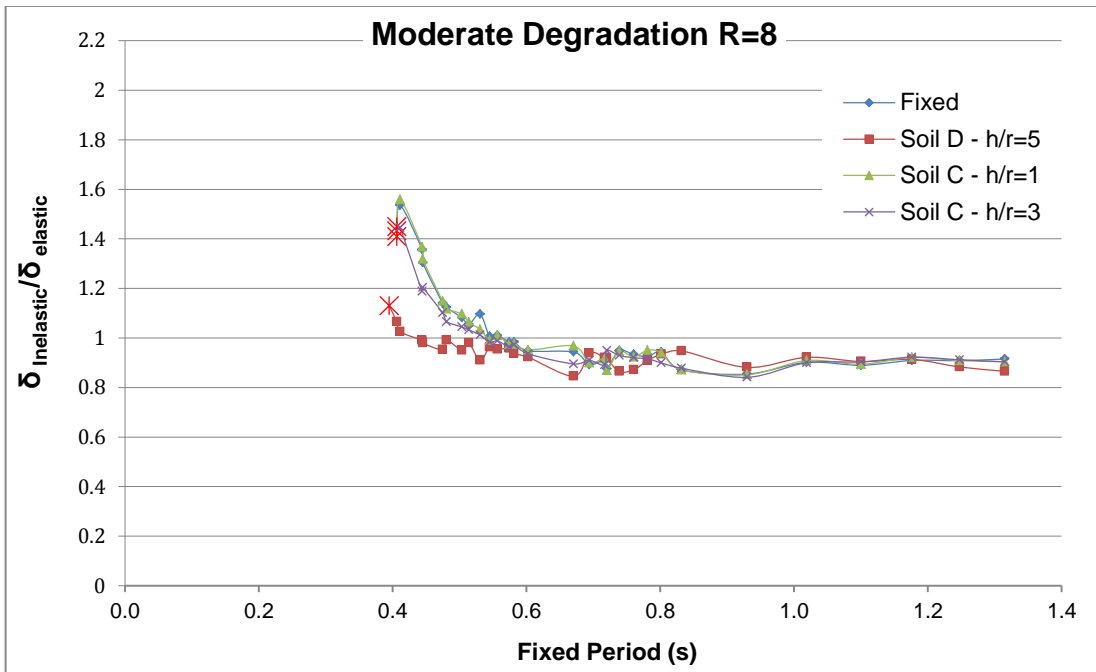
**Figure. 22** Inelastic Displacement Ratio of SDOF RC Columns when R=8

R=3
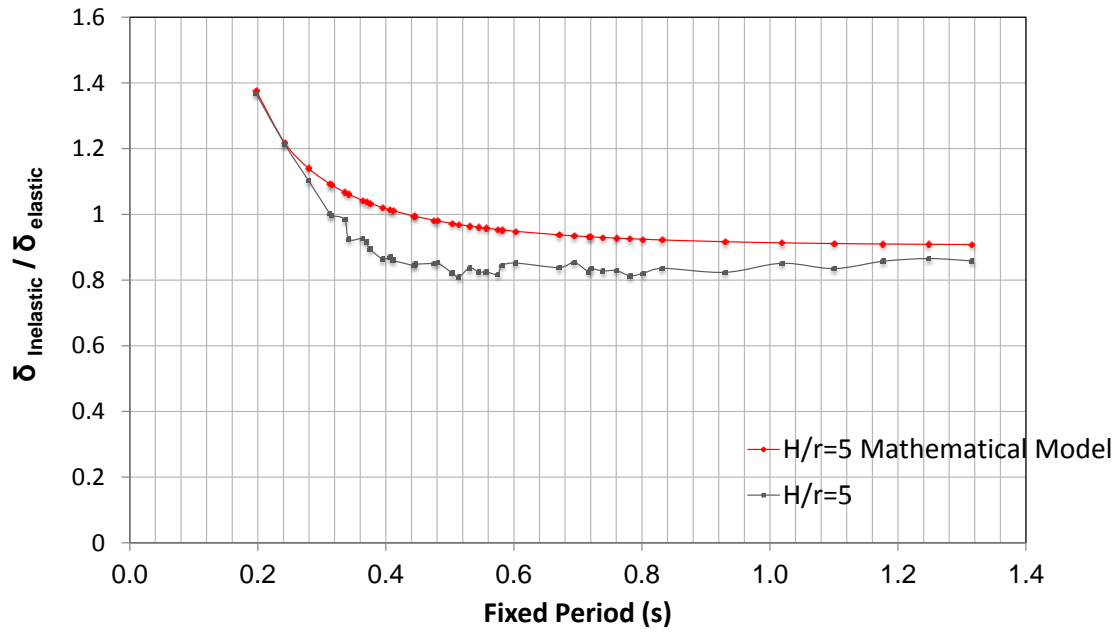
**Figure. 23** Modified Inelastic Displacement Ratio of R=3 for h/r=5

R=4
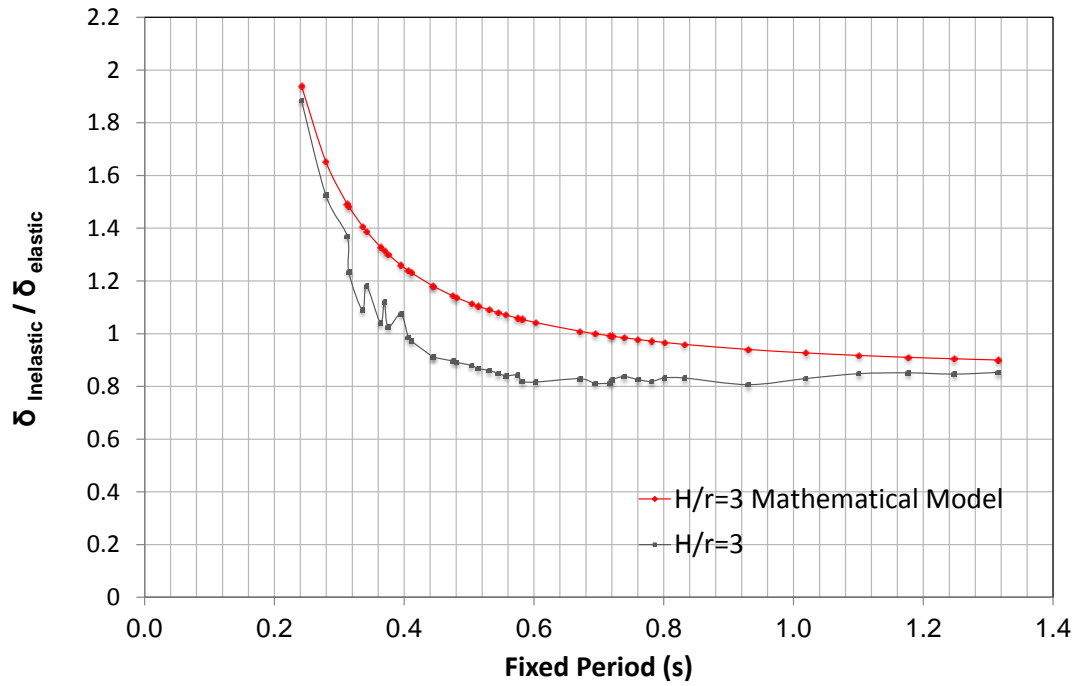
Figure. 24 Modified Inelastic Displacement Ratio of R=4 for h/r=3

R=6
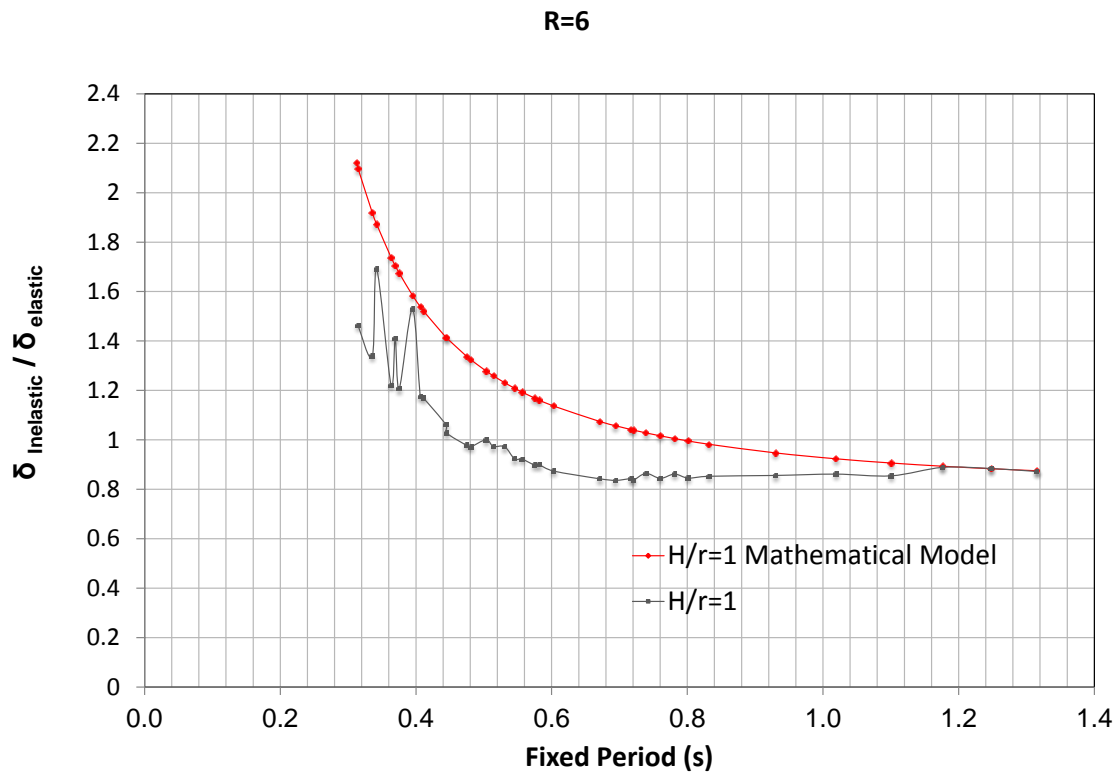
Figure. 25 Modified Inelastic Displacement Ratio of R=6 for h/r=1

R=7
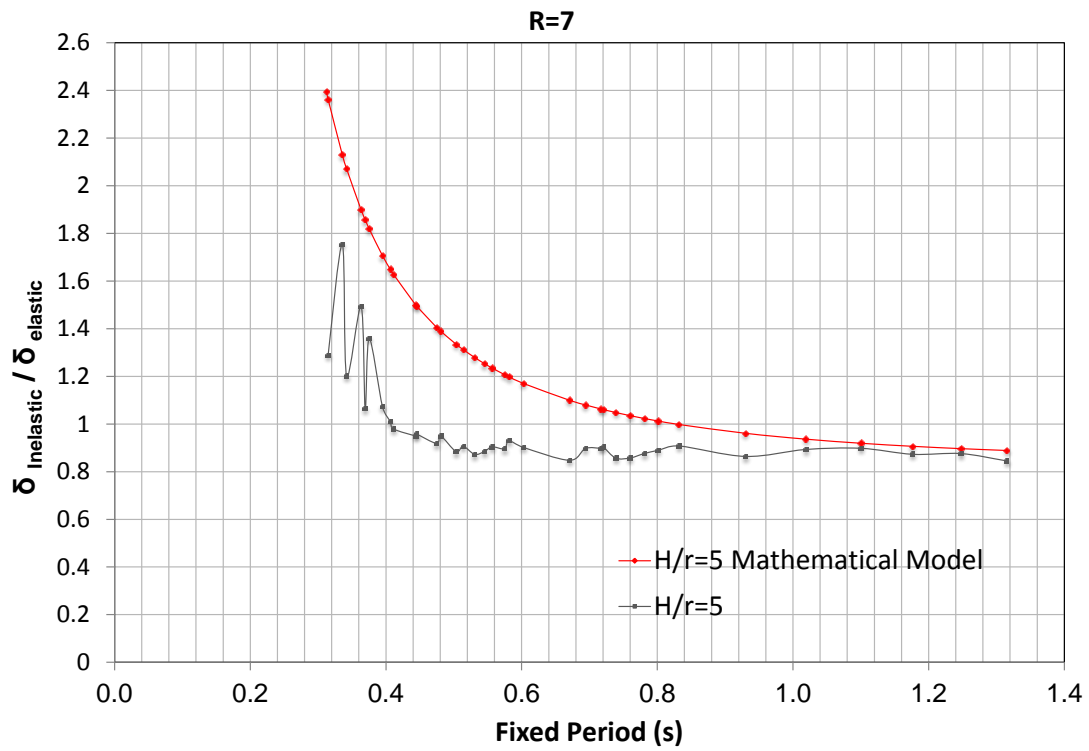
Figure. 26 Modified Inelastic Displacement Ratio of R=7 for h/r=5